

# Discontinuous Galerkin Method for Numerical Simulation of Dynamic Processes in Solids

V. A. Miryaha, A. V. Sannikov, and I. B. Petrov  
 Moscow Institute of Physics and Technology, Moscow, Russia  
 e-mail: vlad.miryaha@gmail.com; petrov@mipt.ru  
 Received September 1, 2014

**Abstract**—This paper examines the application of the Galerkin discontinuous method for deformation and destruction problems of elastic and elastoplastic bodies and combined problems of elasticity and acoustics. It proposes a 2-sided crack model in the problems of destruction, an account of the elastic plastic rheology in the Prandtl-Reuss model, implementation of the dynamic contact of bodies, an algorithm for the joint solution of linear systems of acoustics and elasticity, and in particular, the issues of shelf seismic prospecting, a comparison of the responses for the model of saturated fluid and infinitely thin cracks, and a modeling of perturbations from underwater objects. The method has been implemented to find the wave picture in heterogeneous media and also the solution of deformation problems by the use of high performance computation systems.

**Keywords:** discontinuous Galerkin method, mechanics of deformable solids, high performance computations, acoustics, shelf seismic prospecting, fluid-filled crack, dynamic contact of bodies, destruction

**DOI:** 10.1134/S2070048215050087

## 1. INTRODUCTION

This paper is devoted to a review of the possibilities of a software commutative package based on the discontinuous Galerkin method. This method has a number of positive features [1]; in our view, the main advantage is the possibility to use a high order convergence by spatial coordinates and time due to the wave specifics of the current problems.

## 2. DISCONTINUOUS GALERKIN METHOD ON UNSTRUCTURED TRIANGULAR GRIDS

The system of elasticity equations in matrix form in the two-dimensional case for isotropic space in the tension and speed variables can be written as [2, 3]

$$\frac{\partial u_p}{\partial t} + \frac{\partial(A_{pq}u_q)}{\partial x} + \frac{\partial(B_{pq}u_q)}{\partial y} = 0, \quad (1)$$

where  $u$  is a vector of 5 unknown variables  $u = (\sigma_{xx}, \sigma_{yy}, \sigma_{xy}, v_x, v_y)^T$ . In [4] the linear system of equations of elasticity is written in speed-displacement variables. (1) and further refer to summation by repeating indices.

The eigenvalues (EVs) of matrices  $A_{pq}$  and  $B_{pq}$  are

$$s_1 = -c_p, \quad s_2 = -c_s, \quad s_3 = 0, \quad s_4 = c_s, \quad s_5 = c_p.$$

Let  $R_{pq}$  be a matrix of right-hand eigen vectors of matrix  $A_{pq}$ . The explicit form of matrices  $A_{pq}$ ,  $B_{pq}$ ,  $R_{pq}$  is given in [2, 5]. To construct a numerical scheme, we consider a system of Eqs. (1). The integration domain is divided into triangles  $T^{(m)}$  and numerated. Consider the case when matrices  $A_{pq}$  and  $B_{pq}$  are constant within  $T^{(m)}$ . Within each triangle the solution of system (1) is numerically approximated as  $u_h$  by means of the linear combination of  $\frac{1}{2}(N+1)(N+2)$  time independent polynomial functions  $\Phi_l(x, y)$  of an order not higher than  $N$ , forming the basis with carrier  $T^{(m)}$  and time-dependent through coefficients  $\hat{u}_{pl}^{(m)}(t)$ :  $(u_h^{(m)})_p(x, y, t) = \hat{u}_{pl}^{(m)}(t)\Phi_l(x, y)$ . On the element's boundaries gaps in the numerical solution are toler-

ated. In [6] a modification of this scheme is proposed, when inside each triangle  $T^{(m)}$  the Jacobians  $A_{pq}$  and  $B_{pq}$  are functions of the coordinate and are also decomposed by the system of basis functions  $\Phi_l(x, y)$ . This modification will be important in problems with continuously changing parameters of a medium, whose gradient is high, in the computation on a coarse computation grid.

Multiply (1) by basic function  $\Phi_k$  and integrate by triangular  $T^{(m)}$ :

$$\int_{T^{(m)}} \Phi_k \frac{\partial(u_h)_p}{\partial t} dV + \int_{T^{(m)}} \Phi_k \left( \frac{\partial(A_{pq}(u_h)_q)}{\partial x} + \frac{\partial(B_{pq}(u_h)_q)}{\partial y} \right) dV = 0. \quad (2)$$

Integration (2) by parts yields

$$\int_{T^{(m)}} \Phi_k \frac{\partial(u_h)_p}{\partial t} dV + \sum_{j=1}^3 \int_{(\partial T^{(m)})_j} \Phi_k F_p^{h,j} dS - \int_{T^{(m)}} \left( \frac{\partial \Phi_k}{\partial x} A_{pq}(u_h)_q + \frac{\partial \Phi_k}{\partial y} B_{pq}(u_h)_q \right) dV = 0. \quad (3)$$

The second term of Eq. (2) could not be integrated because of the discontinuity of solution  $u_h$  and matrices  $A_{pq}$  and  $B_{pq}$  on the cell boundary in the general case. This problem is solved by the introduction of the numerical flow function through the edge of triangle  $F_p^{h,j}$ . A great number of possible variants in assignment of a numerical flow are known [1, 7–11]. In our case, it is most reasonable [1, 7, 10] to choose the upwind flux, which reflects the wave process of the system of equations being solved. Finding the upwind flux amounts to solving the problem of the Riemann arbitrary discontinuity decay problem [12]. In our case of the isotropic space, the Riemann multidimensional problem can be roughly reduced to a one-dimensional problem (the *x-split Riemann problem* [8]). In the case of linear systems of hyperbolic equations the Riemann one-dimensional problem has an analytical solution [1, 7]. For the case of the viscosity and acoustics, the Riemann problem is solved in [12].

In (3) behind  $(\partial T^{(m)})_j$  the sides of triangle  $T^{(m)}$  are denoted,  $j = 1, 2, 3$ , and behind  $F_p^{h,j}$  the flux through edge  $j$  of cell  $T^{(m)}$  in the global system of coordinates is given by the following formulas:

$$R_{pq} = \left\{ \left\{ r_i^{(m)} \right\}_{i:s_i^{(m)} < 0}, \left\{ r_i^{(m_j)} \right\}_{i:s_i^{(m_j)} > 0} \right\}, \quad (4)$$

$$u_p^{\text{in}} = (T_{pq}^{m_j})^{-1} \hat{u}_{ql}^{(m)} \Phi_l^{(m)}, \quad u_p^{\text{out}} = (T_{pq}^{m_j})^{-1} \hat{u}_{ql}^{(m_j)} \Phi_l^{(m_j)}, \quad (5)$$

$$\begin{aligned} u_p^\downarrow &= \frac{1}{2} (u_p^{\text{in}} + u_p^{\text{out}}) + \frac{1}{2} R_{pq} \text{diag} \{ \text{sgn}(s_1), \dots, \text{sgn}(s_5) \} R_{pq}^{-1} (u_q^{\text{in}} - u_q^{\text{out}}) \\ &= \frac{1}{2} (u_p^{\text{in}} + u_p^{\text{out}}) + \frac{1}{2} R_{pq} \text{diag} \{ -1, -1, 0, 1, 1 \} R_{pq}^{-1} (u_q^{\text{in}} - u_q^{\text{out}}), \end{aligned} \quad (6)$$

$$F_p^{h,j} = T_{pq}^{m_j} A_{ql}^{(m)} u_l^\downarrow. \quad (7)$$

Here index  $m_j$  corresponds to the triangle neighboring  $T^{(m)}$  through the common side with number  $j$ ;  $T_{pq}^{m_j}$  is the matrix of transition to the system of coordinates of edge (SCE)  $m_j$ , in which axis  $OX'$  is codirected with the outside normal of the edge (see Fig. 1);  $R_{pq}$  is a matrix composed of eigenvectors of matrix  $A_{pq}^{(m)}$ , corresponding to negative EV  $s_i^{(m)}$ , and eigenvectors  $A_{pq}^{(m_j)}$ , corresponding to positive EV  $s_i^{(m_j)}$ ;  $u_p^{\text{in}}$ ,  $u_p^{\text{out}}$  are the limits of the numerical solution on the inside and outside of edge  $j$  of triangle  $T^{(m)}$ , respectively, in CKP  $m_j$  [2];  $u_p^\downarrow$  is the solution of the Riemann one-dimensional problem in CKP  $m_j$  [12]; and  $A_{ql}^{(m)} u_l^\downarrow$  is the numerical flux in SCE  $m_j$ .

Integrating (4), (5), (6), and (7), we obtain the end formula for  $F_p^{h,j}$ :

$$F_p^{h,j} = F_{pl}^{h,\text{in},j} \Phi_l^{(m)} + F_{pl}^{h,\text{out},j} \Phi_l^{(m_j)}, \quad (8)$$

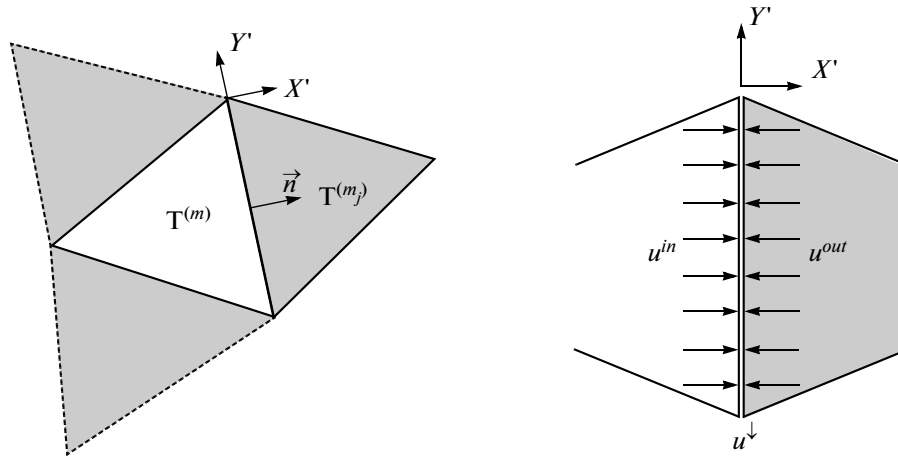


Fig. 1. Element of the calculation grid.

where

$$\begin{aligned}
 F_{pl}^{h,in,j} &= T_{pq}^{m_j} \left( A_{qs}^{(m)} - \frac{1}{2} R_{qt} \left( \Lambda_{tr}^{(m)} - |\Lambda_{tr}^{(m)}| \right) R_{rs}^{-1} \right) \left( T_{sk}^{m_j} \right)^{-1} \hat{u}_{kl}^{(m)}, \\
 F_{pl}^{h,out,j} &= \frac{1}{2} T_{pq}^{m_j} R_{qt} \left( \Lambda_{tr}^{(m)} - |\Lambda_{tr}^{(m)}| \right) R_{rs}^{-1} \left( T_{sk}^{m_j} \right)^{-1} \hat{u}_{kl}^{(m_j)}, \\
 \Lambda_{pq}^{(m)} &= \text{diag} \left\{ -c_p^{(m)}, -c_s^{(m)}, 0, c_s^{(m)}, c_p^{(m)} \right\}, \\
 |\Lambda_{pq}^{(m)}| &= \text{diag} \left\{ c_p^{(m)}, c_s^{(m)}, 0, c_s^{(m)}, c_p^{(m)} \right\}.
 \end{aligned}$$

Similar approaches to the construction of a numerical flux are also used in [4, 13, 14].

After discretization by spatial variables, Eq. (1) assumes the form

$$\begin{aligned}
 \frac{\partial}{\partial t} \hat{u}_{pl}^{(m)} \int_{T^{(m)}} \Phi_k \Phi_l dV + \sum_{j=1}^3 F_{pl}^{h,in,j} \int_{(\partial T^{(m)})_j} \Phi_k^{(m)} \Phi_l^{(m)} dS + \sum_{j=1}^3 F_{pl}^{h,out,j} \int_{(\partial T^{(m)})_j} \Phi_k^{(m)} \Phi_l^{(m_j)} dS \\
 - A_{pq} \hat{u}_{ql}^{(m)} \int_{T^{(m)}} \frac{\partial \Phi_k}{\partial x} \Phi_l dV - B_{pq} \hat{u}_{ql}^{(m)} \int_{T^{(m)}} \frac{\partial \Phi_k}{\partial y} \Phi_l dV = 0.
 \end{aligned} \tag{9}$$

Next, Eq. (9) is integrated by time, for example, by the Runge-Kutta method of a high order of accuracy. By using certain procedures [2] the integrals by basis functions can be calculated beforehand, considerably increasing the efficiency of the scheme. The described scheme allows us to solve the original system of equations with an arbitrary order of approximation by space, actually constrained by no more than machine accuracy. The order of approximation by time is determined by the used integrator and it is also limited only to machine precision.

The conditions of adhesion [4], sliding, and solid friction [13, 15] are taken into account when solving the Riemann one-dimensional problem. The boundary conditions are implemented by means of the method of ghost cells [7] and the Riemann inverse problem.

In this work as a system of basis polynomials the Lagrange polynomials [1] were used. Integration by time was made by means of the Dormand-Prince 7-stage integrator of the 5th order with the time adaptive step. In [2, 13] the ADER scheme is used for integration.

### 3. PARALLEL IMPLEMENTATION OF THE NUMERICAL METHOD

The above-described numerical method is totally local and well suited for parallelization [16, 17]. The method was implemented in [18] using the OpenMP and MPI techniques for calculations on highly productive computation systems. To construct the dependences of acceleration on the number of cores (see Fig. 2) once by means of the library *triangle* [19], a computation grid consisting of  $3.2 \times 10^6$  triangles was

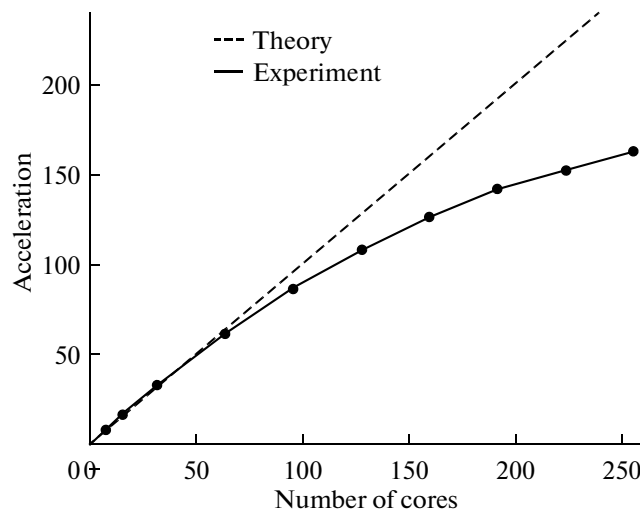


Fig. 2. Dependence of acceleration on the number of cores during the joint use of the OpenMP and MPI technologies.

built, which were then divided into computation domains with the use of the *Metis* library [20]. Polynomials of the 1st order made up basis  $\Phi_j$ .

Computations were performed at the information computation center (ICC) of Novosibirsk State University.

Also, to increase the speed of the software programs in situations where the sizes of triangles are highly varied, a technique of the multiple step by time was used [21–23], implemented for both one-stage and multistage integrators.

#### 4. JOINT TASKS OF ELASTICITY AND ACOUSTICS

There is a rather large class of problems in which it is needed to simulate the contact of viscous and acoustic media: problems of seismic prospecting, defectoscopy, traumatology, earthquake research, and detecting underwater objects. In this work an approach from [4] was used, consisting in analytically solving the Riemann problem on the contact of acoustic and elastic media. This solution turned out to coincide with the solution of the Riemann problem for two contacting elastic media (8), if we assume that the shift module  $\mu = 0$  in matrices  $A_{pq}$  and  $R_{pq}$ . A similar approach is described in [5]. Matrix  $R_{pq}$  in the case of contact, when at least one of the contacting media is acoustic, becomes degenerated. The symbolic computation of the expression  $R_{pq} \left( \Lambda_{ql}^{(m)} - \left| \Lambda_{ql}^{(m)} \right| \right) R_{ls}^{-1}$  from the formula for flux  $F_p^{h,j}$  (8) makes it possible to avoid the 0/0 kind of uncertainty.

**4.1. Shelf seismic prospecting.** Currently, the shelf seismic prospecting in the shelf of the Arctic seas is one of the promising lines associated with the high potential of hydrogen carbons in the Northern regions. The discontinuous Galerkin method allows the use of polynomials of a high order, thereby reaching a high

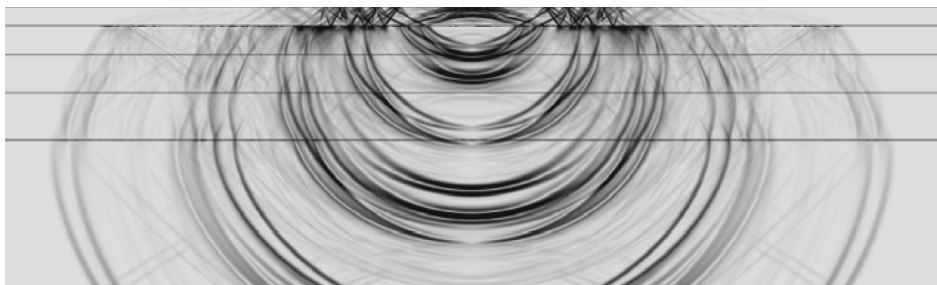


Fig. 3. Wave picture in a multilayer medium.

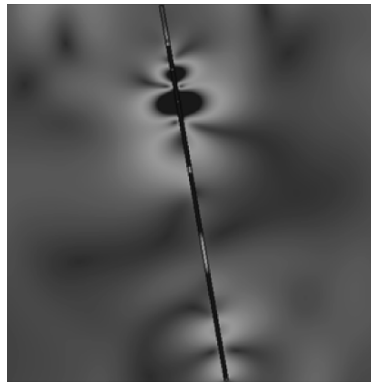


Fig. 4. Krauklis waves in a fluid saturated rift.

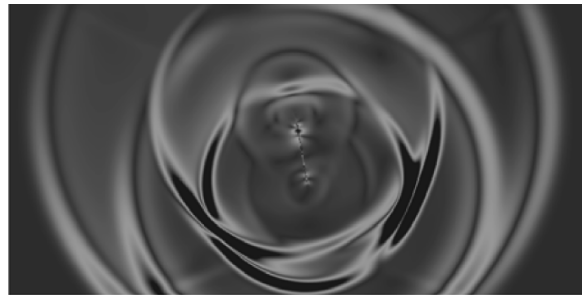


Fig. 5. Response from a fluid saturated rift.



Fig. 6. Response from an infinitely thin crack.

order of convergence by the spatial coordinates, which is critical in modeling wave processes in heterogeneous media, which, in turn, play the key role for the problems of seismic prospecting.

Figure 3 shows an example of the computation of a wave picture initiated by a series of synchronous spherical explosions in a multilayer medium, whose upper layer has acoustic characteristics with the parameters of the water and the rest of the characteristics are elastic ones, corresponding to soils [24].

Figure 3 shows value  $\sqrt{(\partial v/\partial x)^2 + (\partial v/\partial y)^2}$ , where  $v$  is the absolute value of speed to increase the visibility of the image. In the calculation the polynomials of the 8th order were used.

**4.2. Study of a fluid saturated crack model in seismic prospecting.** As a model of oil containing cracks in a numerical study of responses in the problems of seismic prospecting, the model [25, 26] of an infinitely thin fluid saturated crack is used, the main advantage of which is the absence of the need for a high cross partition of the computational grid in the fractured area, which leads to a considerable increase of the computation time. The difference of wave responses from the fluid saturated snap with dimensions of  $1 \text{ m} \times 100 \text{ m}$  (see Fig. 5) and infinitely thin crack (see Fig. 6) was studied at similar time moments. There

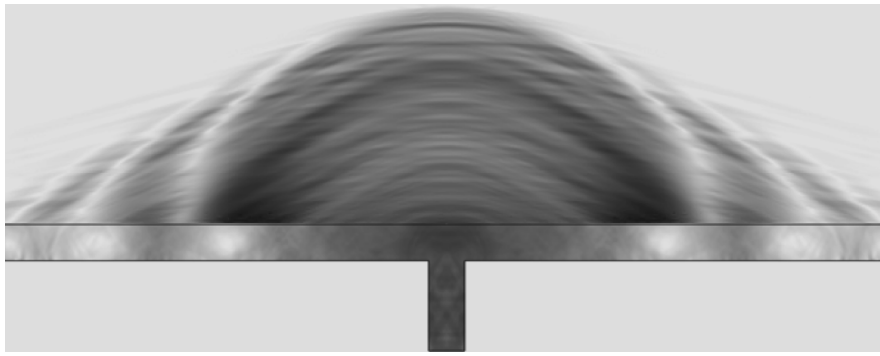


Fig. 7. Wave picture from a low frequency vibration of the object plating.

is a difference in wave patterns, which results from the finite size of the snap in the former. Figure 4 shows the Krauklis waves, typical of a crack of finite size [27]. In the calculation polynomials of the 4th order were used.

In the future, we plan to investigate the effect of the finite size of the crack on the response to the cracks with the ratio of the longitudinal and transverse dimensions of  $1 : 10^3 - 1 : 10^4$  that have been already found in the practical problems of seismic prospecting.

**4.3. Modeling the perturbations from underwater objects.** The spectrum of problems of hydraulic acoustics is large [28]. One of them is the problem of the location of underwater objects, solved by active and passive methods.

In this work we have carried out a numerical modeling of the passive method of detection. We have dealt only with the direct problem of generating a perturbation by the object. Figure 7 shows a wave picture of perturbations in a water column as the result of a low frequency vibration of the object's casing. In the calculation the polynomes of the 4th order were used.

## 5. CALCULATION OF DYNAMIC CONTACT BOUNDARIES

For calculating problems with dynamically changing contact conditions, a method was proposed with the following features:

- The dynamic contact condition is mathematically equivalent to the static in cases of conformal contacts.
- In the absence of a contact, the condition is equivalent to a free boundary.
- In the case of nonconformal contacts, all the basis functions providing for a high order of interpolation are used.

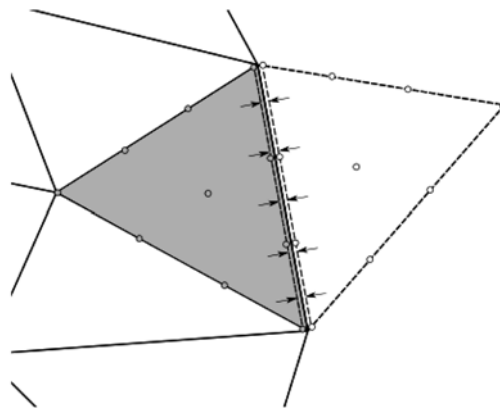
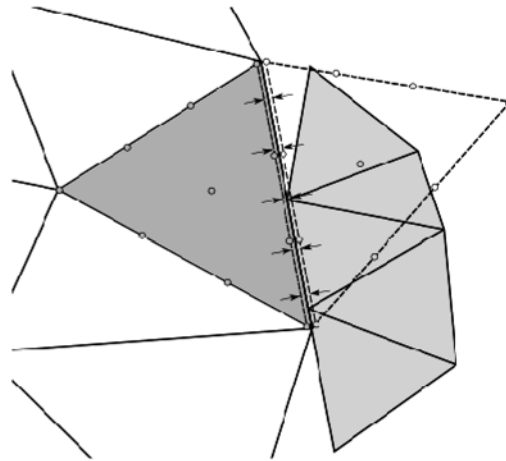


Fig. 8. Imaginary cell.



**Fig. 9.** Construction of the solution in an imaginary cell on the contact boundary.

- The implementation of the method on the Lagrange basis polynomes permits us to avoid high costs for the operations of numerical integration for the deduction of flows on dynamically changing contact boundaries.

In order obtain this mixed contact-boundary condition, it has been found that the method of the free boundary calculation proposed in [2] is mathematically equivalent to the calculation of the contact condition with the imaginary cell [7], conformally connected to the boundary cell, the solution in which is given in a special way, with the use of the solution of the reverse Riemann problem of a discontinuity decay on the boundary. This interpretation is illustrated in Fig. 8.

The solution in the imaginary cell is determined in its basis points marked in Fig. 8 in white based on the known solution in the considered cell in such a way that on the boundary of the imaginary and actual cells the necessary boundary condition is fulfilled. The specific form of the necessary transformation is found, for example, in [1].

In the proposed method of dynamic contacts, this method is extended, but the solution in the basis points of the imaginary cell is built based on the solution in both contacting surfaces (see Fig. 9).

If the reference point of the imaginary cell falls into a cell of the contacting grid, the solution in the reference point is obtained by interpolation in this cell. Otherwise, the solution is taken from the point corresponding to the reference boundary cell. The values in the nodes of the imaginary cell are decomposition coefficients at the basis polynomes, from which at the stage of precalculation it is possible to count the flows through the corresponding facets of the cell. An important feature of this approach is that the preliminary calculations can be used even in a dynamically changing contact boundary due to the fact that the imaginary cell is always conformal with the boundary one.

The developed scheme is equivalent to the scheme of the calculation of static contacts in the case of the conformal disposition of contact cells and the free boundary in the case of the absence of contact,



**Fig. 10.** Slabbing plate.

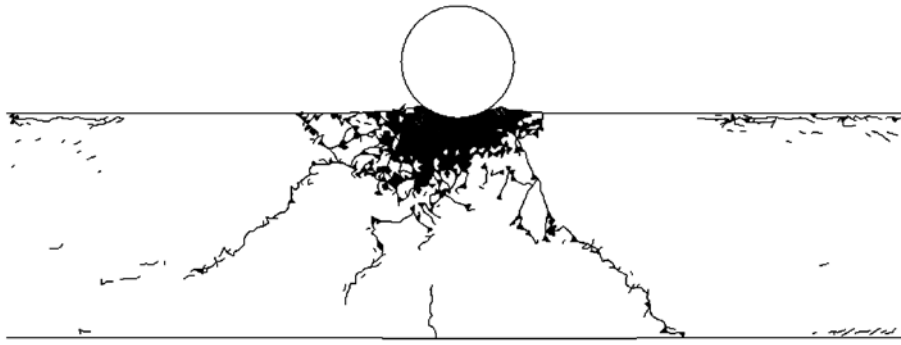


Fig. 11. Result of the numerical modeling of the inclined shock of a metallic ball on glass.

whose properties are now already known in detail. On the other hand, in the case of nonconformal contacts, the proposed scheme is already known to be fairly accurate and effective in the circle of problems to which it has been applied.

## 6. 2-COAST CRACK MODEL IN PROBLEMS OF THE DESTRUCTION OF SOLIDS

The simulation of the deformation of solids with their consequent destruction is an actively developing area of mathematical modeling. In this work, a version of the development of the one-coast crack model proposed in [29], applied in [30, 31], is proposed. Routinely, the two-coast model of a crack is used based on the finite element model (*FEM*) and has received further development (GFEM et al. [32]). A similar technique of the split of the difference grid by nodes with local restructuring is described in [33].

The core of this approach lies in the fulfillment of some criterion of destruction, for example, by the primary stresses for a pair of contacting cells, the contact between them is changed by a pair of free boundaries, which are next modeled independently. Due to the above-described calculation method of dynamic contact boundaries, in the process of calculation, the crack's edges can multiply converge and again diverge. During the collapse of the crack between the two sides, the contact condition (sticking, dry friction, slip) is set again.

The proposed discrete collapse model was combined with the continual model of collapse based on the Mises plasticity criterion [29], reflecting transition into the fractured state. In the separation of an individual cell, when it has a free boundary on each of its sides, it is given the status "crumbled" and the original contacts of adhesion with the neighboring cells are set. The fractured cells cannot counteract the strain and the parameters of these cells are corrected in a special way: if the Lamé parameters before the collapse had had values  $\lambda^0$  and  $\mu^0$ , after the collapse the shift module of the disrupted material was scaled  $\alpha \approx 0.1$  times:  $\mu = \alpha\mu^0$ . The module of the compression of all sides of the material is sustained after the collapse, which allows computation of  $\lambda$  [30].

For a description of the behavior of the investigated material objects, the rheological models of the linear-elastic and elastic-plastic media (Prandtl-Reis model with the Mises and Mises-Shleihert plasticity conditions [30]) were used.

Here is the result of the thrust of a steel bead on glass (Fig. 8) and a similar numerical experiment (Fig. 10), in which the thrust was at an angle of  $10^\circ$  relative to the vertical. Similar pictures can be viewed, for example, when a stone hits the glass of a moving car.

In the numerical experiment the polynomes of the 2nd order were used.

This approach can have advantages, for example, in modeling high speed hits of fragile bodies when the wave effects are considerable or in the calculation times when the crack opening is not small.

## 7. FURTHER RESEARCH

The basic direction for further research is to solve the same problems but now in a three-dimensional statement, which imposes higher requirements on the effectiveness of implementation. It is planned to investigate the problem of regularizing the numerical method [34–36], which is especially appropriate for the simulation of destruction. In [15, 30], variants are proposed in the regularization of the numerical



scheme for modeling the problems of the destruction of solids. It is also planned to use more complicated models of environment destruction.

## 8. CONCLUSIONS

In this work, a numerical scheme is described allowing calculations of acoustic-elastic problems of the wave dynamics of elastic media with inhomogeneous inclusions, complicated dynamic contact boundaries, and dynamic disruptions. This scheme was implemented in a software package recommended for the solution of a number of relevant problems of seismic prospecting, hydro-location, and failure theory and which has proven to be efficient in parallelization in operation on highly productive clusters with a distributed memory.

## ACKNOWLEDGMENTS

The work was financially supported by grant 14-11-00434 from the Russian Research Foundation.

## REFERENCES

1. J. S. Hesthaven and T. Warburton, *Nodal Discontinuous Galerkin Methods: Algorithms, Analysis, and Applications*, Texts in Applied Mathematics, vol. 54 (Springer, 2008).
2. M. Käser and M. Dumbser, “An arbitrary high order discontinuous Galerkin method for elastic waves on unstructured meshes I: The two-dimensional isotropic case with external source terms,” *Geophys. J. Int.* **166**, 855–877 (2006).
3. J. Virieux, “SH-wave propagation in heterogeneous media: Velocity-stress finite-difference method,” *Geophys.* **49**, 1933–1957 (1984).
4. L. C. Wilcox, G. Stadler, C. Burstedde, and O. Ghattas, “A high-order discontinuous Galerkin method for wave propagation through coupled elastic-acoustic media,” *J. Comput. Phys.* **229**, 9373–9396 (2010).
5. M. Käser and M. Dumbser, “A highly accurate discontinuous Galerkin method for complex interfaces between solids and moving fluids,” *Geophysics* **73** (3), T23 (2008).
6. C. E. Castro, M. Käser, and G. B. Brietzke, “Seismic waves in heterogeneous material: subcell resolution,” *Geophys. J. Int.* **182**, 250–264 (2010).
7. R. L. LeVeque, *Finite Volume Methods for Hyperbolic Problems* (Cambridge Univ. Press, Cambridge, 2002).
8. E. F. Toro, *Riemann Solvers and Numerical Methods for Fluid Dynamics*, 2nd ed. (Springer, 1999).
9. J. A. Trangenstein, *Numerical Solution of Hyperbolic Partial Differential Equations* (Cambridge Univ. Press, 2008).
10. E. Sonnendruker, *Numerical Methods for Hyperbolic Systems*, Lecture Notes (Sommersemester, 2013).
11. D. A. di Pietro and A. Ern, *Mathematical Aspects of Discontinuous Galerkin Methods* (Springer, 2012).
12. A. G. Kulikovskii, N. V. Pogorelov, and A. Y. Semenov, *Mathematical Aspects of Numerical Solution of Hyperbolic Systems* (Fizmatlit, Moscow, 2001; Chapman and Hall, CRC, Boca Raton, 2001).
13. C. Pelties, A. A. Gabriel, and J. P. Ampuero, “Verification of an ADER-DG method for complex dynamic rupture problems,” *Geosci. Model Dev. Discuss.* **6**, 5981–6034 (2013).
14. M. Hochbruck, T. Pažur, A. Schulz, E. Thawinan, and C. Wieners, “Efficient time integration for discontinuous Galerkin approximations of linear wave equations” (2013). <http://na.math.kit.edu/download/papers/TI-DG-Wave.pdf>
15. C. Pelties and M. Käser, “Dynamic rupture modelling on unstructured meshes using a discontinuous Galerkin method,” *Comput. Methods Struct. Dynam. Earthquake Eng.*, 3201–3209 (2011).
16. M. Käser, C. Pelties, C. E. Castro, H. Djikpesse, and M. Prange, “Wave field modeling in exploration seismology using the discontinuous Galerkin finite element method on HPC-infrastructure,” *The Leading Edge* **29**, 76–85 (2010).
17. L. Noels and R. Radovitzky, “An explicit discontinuous Galerkin method for non-linear solid dynamics: formulation, parallel implementation and scalability properties,” *Int. J. Numer. Methods Eng.* **74**, 1393–1420 (2008).
18. V. A. Miryaha and A. V. Sannikov, “On the software implementation of the parallel algorithm of discontinuous Galerkin method for numerical modeling of wave processes in heterogeneous solid deformable media,” in *Proceedings of the 56th Scientific Conference of Moscow Physical Technical Institute* (Moscow, 2013), Vol. 2, p. 135.
19. J. R. Shewchuk, “Delaunay refinement algorithms for triangular mesh generation,” *Comput. Geom.: Theory Appl.* **22**, 21–74 (2002).
20. G. Karypis and V. Kumar, “A fast and highly quality multilevel scheme for partitioning irregular graphs,” *SIAM J. Sci. Comput.* **20**, 359–392 (1999).

21. S. Tirupathi, J. S. Hesthaven, Y. Liang, and M. Parmentier, “Multilevel and local timestepping discontinuous Galerkin methods for magma dynamics,” *Geophys. J. Int.*, 1–12 (2013).
22. A. Demirel, J. Niegemann, K. Busch, and M. Hochbruck, “Efficient multiple time-stepping algorithms of higher order,” Preprint, *J. Comput. Phys.* (2014, submitted).
23. I. B. Petrov, A. V. Favorskaya, A. V. Sannikov, and I. E. Kvasov, “Grid-characteristic method using high-order interpolation on tetrahedral hierarchical meshes with a multiple time step,” *Math. Mod. Comput. Simul.* **5**, 409–415 (2013).
24. V. I. Golubev, I. B. Petrov, and N. I. Khokhlov, “Numerical simulation of seismic activity by the grid-characteristic method,” *Comput. Math. Math. Phys.* **53**, 1523–1533 (2013).
25. M. V. Muratov and I. B. Petrov, “Estimation of wave responses from subvertical macrofracture systems using a grid characteristic method,” *Math. Mod. Comput. Simul.* **5**, 479–491 (2013).
26. I. E. Kvasov and I. B. Petrov, “High-performance computer simulation of wave processes in geological media in seismic exploration,” *Math. Mod. Comput. Simul.* **52**, 302–313 (2012).
27. M. Frehner, “Krauklis wave initiation in fluid-filled fractures by seismic body waves,” *Geophysics* **79**, 27–35 (2014).
28. P. C. Etter, *Underwater Acoustic Modelling and Simulation*, 3rd ed. (Spon Press, London, 2003).
29. G. Mienchen and S. Sack, “Numerical method 'Tensor',” in *Fundamental Methods in Hydrodynamics*, Ed. by B. Alder, S. Fernbach, and M. Rotenberg (Mir, Moscow, 1967; Academic Press, New York, London, 1964), p. 185–211.
30. I. B. Petrov and F. B. Chelnokov, “Numerical analysis of wave processes and fracture in layered targets,” *Comput. Math. Math. Phys.* **43**, 1503–1519 (2003).
31. V. I. Golubev, D. P. Grigorievikh, I. B. Petrov, and N. I. Khokhlov, “Evaluation of seismic resistance of dome constructions based on the results of full-wave modeling,” *Int. J. Comput. Civil Struct. Eng.* **10**, 65–71 (2014).
32. M. A. Schweitzer, “Meshfree and generalized finite element methods,” *Habilitationsschrift (Math.-Naturwissensch. Fakult., Rheinischen Friedrich-Wilhelms-Univ., Bonn, 2008)*.
33. A. V. Gerasimov, V. N. Barashkov, V. P. Glazyrin, A. A. Konyaev, M. Yu. Orlov, S. V. Pashkov, V. F. Tolkachev, V. G. Trushkov, and Yu. F. Khristenko, *Theoretical and Experimental Studies of the Interaction of a High-Speed Objects*, Ed. by A. V. Gerasimov (Tomsk. Univ., Tomsk, 2007), pp. 177–187 [in Russian].
34. M. E. Ladonkina, O. A. Neklyudova, and V. F. Tishkin, “Study of the limiter impact on the order of solution accuracy by discontinuous Galerkin method,” Preprint IPM RAN No. 34 (Inst. Prikl. Mat. im. M. V. Keldysha RAN, Moscow, 2012).
35. M. E. Ladonkina, O. A. Neklyudova, and V. F. Tishkin, “Impact of different limiting functions on the order of solution obtained by RKDG,” *Math. Mod. Comp. Simul.* **5**, 346–349 (2013).
36. M. E. Ladonkina, O. A. Neklyudova, and V. F. Tishkin, “Limiter of heightened accuracy order for discontinuous Galerkin method on triangle grids,” Preprint IPM RAN No. 53 (Inst. Prikl. Mat. im. M. V. Keldysha RAN, Moscow, 2013).

*Translated by D. I. Shtirmer*

SPELL: 1. Niegemann, 2. Sannikov